

# NASA Technical Memorandum 100460

## Payload Bay Atmospheric Vent Airflow Testing at the Vibration and Acoustic Test Facility

James D. Johnston, Jr.

February 1988

(NASA-TM-100460) PAYLOAD BAY ATMOSPHERIC  
VENT AIRFLOW TESTING AT THE VIBRATION AND  
ACOUSTIC TEST FACILITY (NASA) 35 pCSCI 01A

N88-18572

Unclas  
G3/02 0130135



National Aeronautics and  
Space Administration

Lyndon B. Johnson Space Center  
Houston, Texas



NASA Technical Memorandum 100460

Payload Bay Atmospheric Vent Airflow Testing  
at the Vibration and Acoustic Test Facility

James D. Johnston, Jr.  
Lyndon B. Johnson Space Center  
Houston, Texas



## CONTENTS

Section		Page
	ABSTRACT	1
1.0	<u>INTRODUCTION</u> .....	1
2.0	<u>TEST SETUP</u> .....	2
2.1	TEST ARTICLE DESCRIPTION .....	2
2.2	WIND TUNNEL CONFIGURATION .....	2
3.0	<u>INSTRUMENTATION</u> .....	3
4.0	<u>OPERATIONAL CHECKOUT OF THE TEST FACILITY</u> .....	3
5.0	<u>SUMMARY OF INITIAL TONE TESTS</u> .....	4
6.0	<u>FINAL TEST PHASE SUMMARY</u> .....	5
7.0	<u>CONCLUDING REMARKS</u> .....	9

## TABLES

Table		Page
I	TEST RUN CHRONOLOGY FOR THE ORBITER VENT BOX .....	10
II	VENT BOX MASS FLOW FOR DIFFERENT OPERATIONAL CONDITIONS .....	13

PRECEDING PAGE BLANK NOT FILMED

## FIGURES

Figure		Page
1	Activity flow for payload bay atmospheric vent testing .....	14
2	Setup for Orbiter vent box wind tunnel tests .....	15
3	Wind tunnel cross-sectional area versus axial station .....	16
4	Air path schematic for VATF wind tunnel showing fixed instrumentation locations .....	17
5	Views of vent box showing instrumentation locations	
	(a) Front view .....	18
	(b) Side views .....	19
6	Microphone array viewed from outside the hemisphere .....	20
7	Velocity profiles across wind tunnel test section .....	21
8	Control of static pressure by duct exhaust height variation .....	22
9	Air velocity versus pressure ratio .....	23
10	Average test section velocity versus compressor output pressure .....	24
11	Vent box tone generation in wind tunnel test at VATF .....	25
12	Overplot of Rossiter and Acoustic modal frequencies versus velocity .....	26
13	Demonstration of dominant vent tone suppression by FRSI flap .....	27
14	Recommended FRSI flap configuration for payload bay vents 3, 4, and 5 .....	28

## ACRONYMS AND SYMBOLS

EMI	electromagnetic interference
FRSI	flexible reusable surface insulation
SFL	Sonic Fatigue Laboratory
VATF	Vibration and Acoustic Facility
dB	decibel
fps	feet per second
Hz	Hertz
lb/sec	pounds per second
scfm	standard cubic feet per minute
psig	pounds per square inch gage





## ABSTRACT

Several concerns related to venting the Space Shuttle Orbiter payload bay during launch led to laboratory experiments with a flight-type vent box installed in the wall of a subsonic wind tunnel. This report describes the test setups and procedures used to acquire data for characterization of airflow through the vent box and acoustic tones radiated from the vent-box cavity. A flexible boundary-layer spoiler which reduced the vent-tone amplitude is described.

## 1.0 INTRODUCTION

Examination of payload bay microphone data from the first few Space Shuttle Orbiter flights disclosed the existence of discrete frequency tones that exceeded payload test criteria for a few seconds during ascent transonic flight. The data coupled with knowledge of appropriate frequencies for cavity tones to exist in the vent boxes were sufficient to conclude that configuration 4 and 5 vent boxes created the tones. In November 1983, Vibration and Acoustic Facility (VATF) personnel were asked to consider laboratory tests to investigate the tone generation. The availability of a configuration 5 vent box acoustic test article, a large compressed air supply at the VATF, and other test equipment at VATF allowed a wind tunnel test setup to be fabricated and installed at low cost. The first test with the vent box mounted to a wind tunnel on January 9, 1985, resulted in generation of a distinctly audible tone, which closely matched existing payload bay flight data in both sound pressure level and frequency. Experiments immediately were turned toward treating the vent box to diminish the tone generation.

Requests for additional testing with the vent box and suggestions for refinements to the test setup resulted in expansion of the original intent of the test program. In addition to the planned tone-reduction experiments, data were needed to document mass flow rates through the vent box and maximum exit velocities from the contamination screen as functions of pressure drop across the vent box and free-stream velocity passing by the vent box external opening. Meetings attended by personnel from the U. S. Air Force, the Aerospace Corporation, the Rockwell International Corporation, and the NASA Lyndon B. Johnson Space Center were held to discuss test priority, facility modifications, and data acquisition requirements. As modifications to the test setup were completed, checkout tests were performed to document facility operational characteristics without the vent box. Finally, a comprehensive series of tests which addressed all the vent box test objectives was conducted from July 2 to August 28, 1985.

Significant direct benefits of the test program included direct measurements of peak velocities through the contamination screen, verification of vent box flow analytical models, and the discovery of a simple technique to reduce vent box tone amplitude during ground tests by using a flap of flexible reusable surface insulation (FRSI) at the upstream edge of the vent box opening. An evaluation of the FRSI flap during Orbiter flight has been recommended to the Orbiter project management. Figure 1 is a timeline of the payload bay atmospheric vent airflow testing at VATF from the original request date through the date of recommendation of an FRSI flap concept flight trial.

## 2.0 TEST SETUP

### 2.1 TEST ARTICLE DESCRIPTION

The vent box used for the VATF test program was representative, in all respects critical for flow tests, to a flight vent box of the vent system number 5 configuration. The test vent box had been used previously as a fixture for an acoustic certification test of an electromagnetic interference (EMI) shield which was installed on the box. A fixed link held the door of the box in an almost fully open position. There was no motor-driven door closure system in the test box. Rockwell International Corporation drawings VT70-384017 and V070-384323 give details of the vent box dimensions and materials.

A rib-stiffened aluminum panel designed to have dynamic similarity with the Orbiter sidewall was provided as a support fixture for the vent. The 30-inch by 68-inch panel represented the Orbiter left side section bounded in the x-direction by a main frame at  $X_o$  979.50 and a stub frame at  $X_o$  1009.75 and bounded in the y-direction by the payload bay longeron and the upper wing surface. The panel, with the vent box attached, was bolted into a frame structure which created a volume around the vent box having geometric similarity with that volume provided by the Orbiter frames and longeron. Provision of a dynamically and geometrically correct support for the vent box allowed for possible structural participation in vent tone generation. Drawing VATF-26022 gives details for the vent box support panel and frame.

### 2.2 WIND TUNNEL CONFIGURATION

Flight data indicated that vent tone generation occurred at high-velocity subsonic conditions; thus, a high-velocity subsonic wind tunnel would be required for laboratory investigations. The existence of a continuous-flow compressed air supply capable of delivering a maximum 50 000 scfm made such a wind tunnel feasible in the VATF. Only a duct was required to receive the available air and conduct it past the vent box opening at an appropriate velocity. The duct had to converge from an area of 6 square feet, required for coupling 16 air supply hoses, to approximately 1 square foot to achieve the desired flow velocity. Noise, vibration, and stability considerations required the duct to be massive. A 13-foot-long acoustic progressive wave test section having a duct area of 72 inches high by 12 inches deep provided an ideal basic structure within which the needed wind tunnel was fabricated from steel structural sections, 3/8-inch-thick steel plate, and wood. The wind tunnel duct has three primary sections: an upstream entrance section which receives air into a 12-inch-deep by 72-inch-high area and converges in a 58-inch length to an area less than one-sixth the initial area; a test section which maintains an area of approximately 136 square inches for a length of 64 inches; and, finally, an exhaust section of 34-inch length which has upper and lower surfaces that are hinged at their connection to the test section to provide a variable exhaust area at the downstream end. The Orbiter vent box was mounted to the test section so that the 7.66-inch high by 23.6-inch long vent opening was in the plane of the test section sidewall, the 7.66-inch-high opening was approximately centered in the test section 13.63-inch height, and the leading edge of the vent box opening was 24 inches aft of the test section upstream end. In the vicinity of the vent box, the test section duct was 10 inches deep (measured normal to the vent opening plane). A schematic representation of the wind tunnel configuration is given by figure 2. Figure 3 provides details of the wind tunnel cross-sectional area as a function of the distance from the leading edge of the vent box opening.

The necessity of detecting and recording possible vent tones during wind tunnel operation required care in locating the wind tunnel to minimize the background noise level outside of the vent box (on the side which normally faces into the Orbiter payload bay). Two sound sources of concern were vibration of the wind tunnel walls and aerodynamic wind tunnel exhaust noise. The vibration problem was obviated by use of massive or stiff duct components. Isolation of vent-box-generated sound from exhaust noise was accomplished by placing the wind tunnel in the Sonic Fatigue Laboratory (SFL) test preparation area and exhausting the wind tunnel into the adjacent reverberant room. The preparation area in which the vent tones were detected is large and acoustically absorptive enough to provide a good anechoic condition for the tone measurement.

### 3.0 INSTRUMENTATION

Definition was required during tests of the vent box of wind tunnel and vent box flow conditions and accompanying vent box sound and vibration response. As many as 76 parameters were simultaneously tape recorded for test runs; other measurements such as temperatures and barometric pressure were manually logged intermittently during test operations. Several figures are used to convey location and usage of different transducers. Figure 4 gives the location of transducers directly associated with defining wind tunnel operational characteristics. Ten fixed-pressure transducers and the microphone (M4) were flush mounted in the duct surfaces. Two cross-sectional planes within the duct could be continuously mapped (point by point measurements) for static pressure and total pressure distribution; a forward probe plane and an aft probe plane were located 2.25 inches upstream and 37.54 inches downstream, respectively, from the leading edge of the vent box opening. Figures 5(a) and 5(b) show the locations of 20 pressure ports and 1 microphone (M2) inside the vent box, of 3 accelerometers surface mounted outside the downstream wall of the vent box, of 2 microphones (M1 and M3) outside the box. In addition to the 4 microphones defined previously, 30 microphones (M5 to M34) were located on the surface of a hemisphere as illustrated in figure 6. This array of microphones permitted source power output and directionality computations for the vent tones.

Two probe devices were used to measure velocities of flow exiting the vent box through the EMI shield and the contamination screen. A manually moved probe (Kurz model 443) provided direct meter readings of the air velocity at selected points outside the EMI shield and contamination screen. Readings were logged manually. An electronic manometer and pitot probe which had a voltage output proportional to air dynamic pressure was used in conjunction with a motor-driven traversing system to make continuous recordings of dynamic pressure of air exiting the contamination screen along selected lines.

### 4.0 OPERATIONAL CHECKOUT OF THE TEST FACILITY

Operational checkout tests of the wind tunnel test facility prior to installing the vent box were performed to identify any unforeseen hazards to personnel or the test article and to determine operational characteristics and limitations for consideration in planning tests using the vent box. Two test phases were conducted with significantly different setup features; therefore, separate checkout test procedures were performed before each phase.

Initial checkout tests of the wind tunnel setup were performed December 4 and 5, 1984. At that time, vent box tests were planned solely to investigate tone generation. The setup requirements for such testing were considerably simpler than those eventually needed for airflow testing. Instrumentation included only microphones M1 to M4, 2 static pressure measurements, 12 total pressure measurements, 2 temperature measurements, and a Kurz air velocity probe. The

main concerns during the first wind tunnel operation were tunnel structural integrity, quietness of operation, and the maintenance of test section static pressure near ambient to prevent excessive flow through the vent box. During the first tunnel operation, for which full flow was gradually achieved, a plate was used to close the vent box mounting area; the run was characterized by little vibration of the test setup, a relatively quiet sound pressure at microphone position M1 of 112 dB, a test section pressure of +0.3 psig, and a maximum flow velocity of about 800 fps. For the second operational configuration, a non-flight-configuration dummy vent box was installed to permit prediction of the wind tunnel operational characteristics to be expected with the flight-type vent. When full compressor flow was approached for this setup, audible tones were emitted by the dummy vent and microphone M1 indicated 128 dB. At a test section velocity of about 800 fps, the test section static pressure was nearly atmospheric and the flow through the vent opening was about 7.5 lb/s. This flow rate was about twice the maximum rate predicted for an Orbiter vent, but the dummy vent box had no contamination screen to restrict flow and the highest expected Orbiter flows occur in rarefied air at much higher velocities. Therefore, testing was initiated using the flight-configuration vent box for tone-generation experiments, which began December 9, 1984.

Requests for additional tone evaluation data and measurement of flow velocities through the contamination screen for various pressure drops across the vent box required significant modifications to the wind tunnel setup. The initial tone evaluation test series was interrupted for refurbishment of the wind tunnel to achieve its final configuration, which is described in section 2.0 of this report. Modifications to the original setup included (1) wooden fairings to lengthen the constant-area test section and provide better area convergence to achieve more uniform cross-sectional flow, (2) cross-sectional pitot-static probe capability upstream and downstream of the vent opening to allow mass flow accounting and evaluation of the tunnel flow smoothness, (3) a continuous probe-traversing system to permit measurement of peak velocities and mass flow through the vent box contamination screen, and (4) hinged upper and lower bounding boards aft of the vent box opening to allow control of the exit area and, thus, of the pressure drop across the vent box.

Upon completion of the previously described modifications, final wind tunnel checkout tests were conducted from May 8 to May 31, 1985. These checkout tests were designed to provide an assessment of cross-sectional flow smoothness, to investigate methods of varying the test section static pressure with respect to ambient room pressure, and to develop a facility operational method to permit repeating run velocity conditions. The data of figure 7, which were obtained by traversing across the wind tunnel just upstream from the vent box opening, show relatively smooth velocity conditions existing in the duct. Figure 8 demonstrates that significant variation could be achieved in the differential pressure across an open vent box. The data shown were obtained with the dummy vent box by varying the exhaust opening size from 13.8 inches to 16.2 inches; two airflow velocity cases, 350 fps and 770 fps, are shown. Operational repeatability of run velocity was obtained by use of data from figures 9 and 10. Figure 9 is a plot of the velocity of compressible air at 86° F versus the ratio of static pressure to total pressure in the flow field. The static and total pressures were monitored at a measurement point in the upstream test section probe plane which was approximately representative of the average cross-sectional velocity. Usually, air compressor output was varied according to the data of figure 10 to provide an approximate desired velocity at the test section measurement point. When more accurate test section velocity was needed, the ratio of static to total pressure was set by variation of compressor output flow to produce the desired wind tunnel velocity in accordance with the data of figure 9.

## 5.0 SUMMARY OF INITIAL TONE TESTS

As related in section 4.0 of this report, initial checkout test results on December 4 and 5, 1984, with a dummy vent box were favorable for beginning tests with the flightlike Orbiter vent

box. On January 9, 1985, the first test using the Orbiter-type vent box and a wind tunnel flow velocity of approximately 800 fps resulted in a strong audible tone having a sound pressure level of 133 dB at microphone position M1 and a frequency of about 300 Hz. This result corresponds well with flight data from the Orbiter payload bay in both amplitude and frequency. Figure 11 gives the power spectrum of the sound measured at microphone position M1 2 feet from the vent contamination screen. A distinct primary tone can be seen to exist at 300 Hz. Evidence of secondary tones can be seen at frequencies higher and lower than the primary tone. Most of the tones observed are readily identifiable as members of an infinite series of tones generated by boundary-layer disturbances over the vent box external orifice. The frequencies of such tones were expressed by Rossiter as

$$f_N = (C/W)(N - \alpha)[1 + 0.2(U/C)^2]^{-0.5} + (1/K), N = 1, 2, 3 \dots$$

where  $C$  is the free-stream speed of sound and  $U$  is the free-stream flow speed over an opening of length  $W$ . Experiments have determined the proper values of  $\alpha$  and  $K$  to be 0.25 and 0.57, respectively, at Mach numbers greater than 0.5. The most intense tones developed within cavities in a flow field occur when Rossiter frequencies coincide with acoustic mode frequencies of the cavity. Such coincidence of longitudinal acoustic modal frequencies and Rossiter frequencies for the vent box can be identified by overplotting the expressions for each as functions of flow velocity. The appropriate expression for the longitudinal acoustic mode frequencies of the vent box is

$$f_i = i(C/2L)[1 + 0.2(U/C)^2]^{0.5}, i = 1, 2, 3 \dots$$

where  $L$  is the vent box longitudinal dimension. Figure 12 is an overplot of the first four Rossiter frequencies with the first two acoustic frequencies versus free-stream velocity. At 800 fps, the first four Rossiter frequencies are 126 Hz, 294 Hz, 462 Hz, and 630 Hz; tones corresponding to these frequencies can be readily identified in the figure 11 data. Extraneous tones of a lower amplitude in figure 11 must indicate higher frequency vent box modes or modal frequencies of the wind tunnel. Previous experimenters have reported that the second Rossiter tone usually predominates. This prediction was found to be the case with the Orbiter vent box; the second Rossiter tone coupled with the first longitudinal acoustic mode to produce the lightly damped (narrow bandwidth) tone at about 300 Hz seen in figure 11.

Immediately following the first exposure of the flight-type vent box to the laboratory flow environment, a visual inspection revealed a 6-inch-long tear in the first pleat of the contamination screen adjacent to the downstream vent box wall. The test run had lasted about 15 minutes, during which a mapping of the flow exiting the contamination screen and the EMI shield was accomplished using the Kurz hand-held velocity probe. Evaluation of the probe data showed that the mass flow rate during this test was approximately 3.6 lb/s through the contamination screen and 0.7 lb/s through the EMI shield. After removal of the contamination screen from the vent box, a more thorough inspection revealed several additional small tears. The tears were repaired by application of a silicone adhesive.

Since the contamination screen was expected to be unavailable for several days to enable inspection and repair, a trail run was conducted at 800 fps without the screen to evaluate the effect on tone generation created by the absence of the screen. The data without the screen were comparable to the data of figure 11 with the screen except that a great amplitude increase occurred in a 100-Hz tone associated with the first Rossiter tone driving a wind tunnel longitudinal mode. Based on the continued existence of an intense 300-Hz tone in the absence of the contamination screen, the decision was made to proceed with an initial series of tests aimed at investigating means of

attenuating the offensive 300-Hz vent tone without the contamination screen mounted to the vent box.

Thirty-six test runs were conducted in this initial vent tone investigative effort without the presence of the contamination screen. Trials at various wind tunnel velocities showed that flow through the open vent box could be reduced considerably without much decrease in tone amplitude by operating in the speed range of 620 fps to 660 fps; this speed range became an operational standard for the initial tests. Tests were conducted to examine the effect on vent tone amplitude produced by rudimentary alteration of several potential tone source parameters including box wall vibration, boundary flow across the box opening, and rotational flow within the box. Additionally, attempts were made to absorb the sound after its creation by the source. The vent box walls vibrate intensely during tone generation. Restraint of the vibration, however, showed it to be a response rather than a tonal generation parameter. The application of baffles oriented to block some of the rotational flow within the vent box and to partially interfere with the longitudinal acoustic modes had a noticeable beneficial effect at selected tonal frequencies. Lining the vent box with acoustically absorptive foams below the vent box door provided good reduction of some tonal components. Whenever the application of a foam tended to block flow to the cavity above the open vent door, however, a tonal component associated with the third Rossiter frequency dramatically increased in sound level. Several experiments involved interfering with the boundary-layer flow at the upstream lip of the vent box. Specific boundary-layer-disturbing configurations tried included covering the opening with 1/4-inch mesh hardware cloth, placing the end of a board perpendicular to the opening and slightly protruding into the boundary layer from inside the vent box, and lining the upstream edge of the vent box with short streamers. All of the methods which directly interacted with the boundary layer effectively reduced most tonal components and had no adverse effects at any dominant frequency. The 1.5-inch-long streamers made of duct tape performed the best overall and provided 12.5 dB of attenuation at the primary 300-Hz tone.

The initial efforts reported in this section to attenuate the vent box tone generation were regarded as providing preliminary information for use in final tests to be conducted after implementation of refinements in the wind tunnel configuration and in operational control of flow conditions past and through the vent box. Also, subsequent tests would include the contamination screen in the vent box setup.

Based on the results of the initial tone attenuation testing, additional experiments were seen to be needed to define the potential attenuation attainable by application of absorptive materials, flow baffles, and boundary-layer disturbers in ways which are compatible with flight usage of the vent boxes and which precipitate minimal engineering efforts for retrofit.

## **6.0 FINAL TEST PHASE SUMMARY**

Multiple objectives were addressed by the final phase of VATF Orbiter vent airflow testing, which occurred from July 2 to August 28, 1985. A chronological summary of the final test phase activity is provided by table I. As seen in table I, there were 105 separate data tape runs for which as many as 76 signals were recorded from microphones, accelerometers, pressure transducers, and a traverse position indicator. Test configuration numbers were assigned to distinct operating conditions of the wind tunnel or vent box setup. Primary operational conditions which defined a configuration were the flow velocity within the test section and the height of the wind tunnel exit plane. Variation of the exit height was used to modify the pressure drop across the vent box and, as a result, the ratio of mass flow through the vent box relative to the test section total mass flow. To indicate relatively the flow through the contamination screen from the wind tunnel, a single reference velocity was measured, when convenient, with the Kurz probe at a point which was 1 inch

outside the contamination screen, 1 inch from the downstream edge, and vertically centered in the upper screen section. The comments column of table I indicates the general objective addressed by each test configuration or identifies runs for which objectives were compromised by anomalies. Test activities were conducted to investigate flow distribution through the vent box, reduction of peak flow through the contamination screen, effectivity of a baffle board on the payload bay side of the contamination screen, sound-generation properties of the vent box, and suppression of the vent box tones.

When the final test phase began, the highest priority objective was to obtain flow distribution data from which contamination screen pressure drop and flow resistance properties and the peak velocity through the screen could be assessed. The data obtained were to be analytically fitted by Aerospace Corporation personnel so that the sea-level test data could be used for predicting flight conditions. Test configurations 5 to 22 were devoted to acquiring the needed flow distribution data, which were tape recorded as runs 7 to 34. For these runs, signals from all fixed-pressure transducers identified in section 3.0 of this report were recorded as well as dynamic pressure traverse data for flow exiting the contamination screen (Orbiter inboard direction). The traverse data were acquired by recording the electronic manometer output while moving a pitot-static probe continuously along six horizontal lines across the contamination screen at distances of 1 inch, 11 inches, or 21 inches between the screen and the probe. For each configuration, additional data for flow through the EMI shield were logged manually from direct Kurz probe indications at 14 points in a plane 1 inch outside the shield. Data from the 6 traverse lines across the contamination screen and from discrete measurement points outside the EMI shield were used to compute approximate total mass flows through the screen and the shield. Table II summarizes key data and computed results from runs for which sufficient data were acquired to permit the mass flow computations. As shown by table II, total mass flows through the vent box ranged from approximately 0.9 to 4.3 lb/s.

The traverse data acquired during the flow distribution investigative runs showed a predominant peak velocity exiting the contamination screen adjacent to the vent box downstream wall. Since such localized high-velocity flow could impinge on and damage payloads, reduction of the peak was explored in several test runs. Initially, a minimal modification was tried which consisted of blocking airflow through the first pleat of the contamination screen by the application of tape. This approach seemed promising because only a single layer of screen material opposed the flow impingement at the first pleat. Data from configuration 43 with and without tape blocking the first pleat indicated virtually no reduction of the peak velocity caused by the tape application. Runs 72, 96, and 97 were conducted later employing a sheet metal deflector installed vertically at the downstream edge of the contamination screen and protruding inward at a 45° angle with respect to the screen surface. Deflectors 3 inches, 2 inches, and 1 inch wide (runs 72, 96, and 97) reduced the peak undeflected velocity of 52 fps (run 73) to 0 fps, 19 fps, and 41 fps, respectively. Thus, deflectors could be employed to good advantage at the downstream edge of the contamination screen. A summary of flow distribution data for the deflection study runs is included in table II.

In preparation for subsequent and sound-suppression effort and to provide knowledge applicable to the Orbiter flights, several test runs were devoted to providing an understanding of the vent box sound-generation characteristics; specific characteristics of interest were sound power output, directionality of the radiated sound, and the effects of wind tunnel speed and mass flow through the vent box on the radiated sound intensity. Generally, the radiated sound intensity was found to increase with wind tunnel flow speed. A speed of 660 fps was selected as a standard for forthcoming sound-suppression work because the vent tone was well developed at this speed and because higher speeds, although yielding greater tone intensity, would have more potential for fatiguing the vent box components. At 660 fps, the tonal intensity increased as the mass flow through the vent box decreased. Decreased mass flow through the vent box accompanied increased wind tunnel height at the exit plane to about 29 inches, where the occurrence of exhaust flow

separation caused an increase of mass flow. An exit height of about 26 inches provided nearly minimum mass flow with a stable exhaust condition and, consequently, was chosen for follow-on noise-suppression work. A hemispherical array of 30 microphones at a 3-foot radius (fig. 6) was used to provide data which would allow tonal power computations and would indicate the directionality of sound radiated from the contamination screen. A review of data from the hemispherical array showed the sound radiation to be dipole; maximum sound was radiated forward and aftward (along the Orbiter x-axis), and a sound minimum tended to exist on a vertical plane through the center of the vent box. This type of radiation pattern would be expected from the vent box first longitudinal acoustic mode, which couples with the external flow boundary layer to generate the dominate vent box tone.

Plates which are 35.75 inches by 29.50 inches (approximately 12 inches larger in both dimensions than a contamination screen) have been used on some Orbiter flights to shield payloads from air loads created by flow through the vent boxes into the payload bay. The baffle plates are centered with respect to the contamination screens in a plane 10 inches from the screens. Test configurations 12, 14, 15, and 23 were dedicated to documenting the flow effects of a baffle board. The Kurz probe was used to measure the distribution of air velocity around the periphery of a 3/4-inch-thick plywood board sized and placed to simulate a flight baffle board; air velocities departing the board edges in the plane of the board were logged for wind tunnel flow speeds of 200, 350, and 500 fps. Obviously, the baffle boards do a good job of shielding objects in the payload bay cargo space from the vent box air inflow. Microphone data from the hemispherical array were tape recorded in configuration 83, run 98, to determine whether the presence of a baffle board would act, also, as an acoustic shield for payloads. Comparison of the array sound levels with and without the simulated baffle board indicated that a baffle board would not be suitable as a sound shield. Whereas the average effect of the board was to reduce the array sound level by 3 dB, some microphones directly shielded by the board actually showed increased levels compared to microphones not being shielded. The laboratory results are considered to be compromised by sound reflections from one wall and the floor and, therefore, to be not closely representative of a flight baffle configuration. Nevertheless, it can be readily concluded that a baffle board would have little merit as a payload sound shield.

More than half of the final test phase experiments, 57 of 105 data runs, directly supported an effort to suppress the vent box tone generation. The noise-suppression experiments were performed at a wind tunnel average cross-sectional airspeed of 660 fps (approximately Mach 0.62) with the contamination screen installed on the vent box and the wind tunnel exit height set at 25.8 inches; these setup parameters resulted in an approximate airflow through the vent box of 1.8 lb/s. Various sound-suppression techniques were applied to the vent box for testing. In an effort to decouple the first longitudinal acoustic mode of the vent box from the boundary tones, two vertical partitions were installed to divide the vent box into three equal subvolumes without interfering with door closure. With the partitions, the predominant tone decreased by only 2.5 dB. Absorption of the acoustic energy within the vent box was attempted by lining the interior wall surfaces with FRSI blankets from 0.5 to 1.25 inches thick; FRSI was used because it has sound-absorptive qualities and is a flight-approved material. Several pounds of FRSI provided just 3.5 dB reduction of the primary tone. Together, the FRSI and partitions provided a marginally acceptable 6-dB attenuation, but the material weight added and the major design effort needed to implement these modifications for flight appeared to be unacceptable for such marginal benefit. Two noise-suppression techniques were applied directly to the boundary-layer noise-generation mechanism. Several shear-layer spoiler configurations which have been used successfully in the past were applied just upstream of the vent box opening on the wind tunnel wall. The externally applied spoilers, being no more than 6 inches long and 1 inch high, were lightweight and small but afforded from 11.5 to 16 dB of attenuation for the major vent tone. Even though they would give excellent noise reduction if implemented, the analysis, the development, and, possibly, the aerodynamic testing required to add spoilers of the standard type to the Orbiter would be expensive. As mentioned in section 5.0 of this



report, 1.5-inch-long duct tape streamers were found to be effective in spoiling the boundary layer and, consequently, in reducing the vent noise. This concept was developed further during the final vent box test phase by use of FRSI to make the streamers. For the wind tunnel tests an 8-inch-long blanket of either 0.16- or 0.32-inch-thick FRSI was positioned to overlap the upstream edge of the vent opening by 1.5 inches; seven 1.5-inch slits 1 inch apart and parallel with the vent x-axis were made to create six adjacent streamers. In several tests with different FRSI samples, attenuation of the dominant vent tone ranged from 7.5 to 13 dB. Figure 13 contains data from one of the FRSI tests. The FRSI streamer approach to vent tone attenuation appears promising for several reasons: good attenuation is achieved with negligible weight; FRSI is an approved thermal protection system material for use on the Orbiter; and little or no design and analysis will be required to implement FRSI streamers. A suggested implementation method for Orbiter vents number 3, 4, and 5 is provided in figure 14.

Extensive data from the final vent box test phase have been given to interested organizations. The size of the base prevents full publication; therefore, the existing data plots, tabulations, and analog magnetic tapes will be retained at the VATF for dissemination upon request. Tables I and II provide a good overview of the tests accomplished and, thus, will provide assistance for formulating data requests.

## 7.0 CONCLUDING REMARKS

As a result of several concerns related to venting the Orbiter payload bay during launch, an experimental program was conducted in the VATF from January 9 to August 28, 1985. For the tests, a configuration 5 vent box was mounted in the wall of a wind tunnel; airflow through the vent box and the sound emitted by the vent box were measured for various wind tunnel operating conditions. Significant direct benefits of the test program included direct measurements of peak velocities through the contamination screen, verification of vent box flow analytical models, and the discovery of a simple technique to reduce the vent box tone amplitude during ground tests by use of a flap of FRSI cut into streamers and overhanging the upstream edge of the vent opening. An evaluation of the FRSI flap during Orbiter flight has been recommended to the Orbiter project management.

The final phase of the vent box test program with the flight-type configuration 5 vent box consisted of 105 test conditions with as many as 76 transducer signals tape recorded. A very large volume of data has been accumulated; therefore, rather than attempting to publish all the existing data plots, tabulations, and analog magnetic tapes, the VATF will retain them for dissemination upon request.

TABLE I.- TEST RUN CHRONOLOGY FOR THE ORBITER VENT BOX

Date	Test Config. no.	Tape run no.	Duct velocity fps	Exit height in	Ref. velocity fps	Comments
7/2/85	1	1,2	200	15		Traverse probe not functional.
7/3/85	2	3,4	200	13.9		Traverse probe not functional.
	3	5,6	200	11.5		Traverse probe not functional.
7/8/85	4		200	11.5		Diagnosing probe system.
7/10/85	5	7	200	11.5	55.0	Complete flow mapping.
	6	8	200	13.1	36.7	Complete flow mapping.
	7	9	200	15	23.3	Complete flow mapping
	8		350	15.5		Air compressor shutdown.
7/11/85	9	10	350	15.5		Data tape recording.
		11	350	15.5	31.7	Contamination screen traverse: 1 inch away.
	10	12	350	13.9		Data tape recording.
		13	350	13.9	63.3	Contamination screen traverse: 1 inch away.
		14	350	13.9		Contamination screen traverse: 1 inch away.
	11	15	350	13.1		Data tape recording.
		16	350	13.1	70.8	Contamination screen traverse: 1 inch away.
		17	350	13.1		Contamination screen traverse: 1 inch away.
	12		350	13.1		Flow mapping around baffle plate.
7/12/85	13	18	350	15		Data tape recording.
		19	350	15	48.3	Contamination screen traverse: 1 inch away.
	14		200	11.5		Tufts at vent opening and contamination screen.
	15		200	11.5		Tufts, mapping baffle plate flow.
	16	20,21	500	16.2		Data tape recording.
		22	500	16.2	45.8	Contamination screen traverse: 1 inch away.
7/17/85	17	23	500	16.9		Data tape recording.
		24	500	16.9	44.2	Contamination screen traverse: 1 inch away.
	18	25	500	18		Data tape recording.
		26	500	18	32.5	Contamination screen traverse: 1 inch away.
	19		500	19.2	24.0	Reference velocity measurement only.
	20	27	500	20		Data tape recording.
		28	500	20	22.5	Contamination screen traverse: 1 inch away.
7/18/85	21	29	500	15		Data tape recording.
		30	500	15	73.3	Contamination screen traverse: 1 inch away.
	22	31	500	13.8		Data tape recording.
		32	500	13.8	98.3	Contamination screen traverse: 1 inch away.
		33	500	13.8		Contamination screen traverse: 11 inch away.
		34	500	13.8		Contamination screen traverse: 21 inch away.
	23		500	13.8		Baffle plate flow mapping.
7/25/85	24	35	750	17.5		Sound directivity.
7/26/85	25	36	700	20		Directivity without contamination screen.
	26	37	700	20		Vent box flow and direction without screen.

TABLE I.- Continued

Date	Test Config. no.	Tape run no.	Duct velocity fps	Exit height in	Ref. velocity fps	Comments
7/29/85	27	38	700	24.2		Vent box flow and direction without screen.
7/31/85	28	39	660	15.5	75.0	Sound o/p vs. mass flow/traverses.
	29	40	660	16.2	69.2	Sound o/p vs. mass flow/traverses.
	30	41	660	14.5	96.7	Sound o/p vs. mass flow/traverses.
	31	42	660	13.8	116.7	Sound o/p vs. mass flow/traverses.
	32	43	660	17.5	56.7	Sound o/p vs. mass flow/traverses.
	33	44	660	20	40.8	Sound o/p vs. mass flow/traverses.
	34	45	660	24.2	75.0	Sound o/p vs. mass flow/traverses.
8/1/85	35	46	660	20		Three directivity conditions.
	36	47	580	20	20.0	Sound o/p vs. mass flow/traverses.
	37	48	580	22	26.7	Sound o/p vs. mass flow/traverses.
	38	49	580	21	20.8	Sound o/p vs. mass flow/traverses.
	39	50	580	18.8	25.8	Sound o/p vs. mass flow/traverses.
	40	51	580	18	33.3	Sound o/p vs. mass flow/traverses.
	41	52	580	17	51.7	Sound o/p vs. mass flow/traverses.
	42	53	580	15.9	70.0	Sound o/p vs. mass flow/traverses.
8/2/85	43		350	13.2		Flow deflection-tape screen pleat.
8/12/85	44	54	660	20	183.3	Anomaly/flow blockage-duct exit.
	45	55	660	20	70.8	Complete contamination screen traverse.
		56	660	20		Sound directivity - 34 microphones.
8/13/85	46	57	660	22	43.3	Sound o/p vs. mass flow/traverses.
	47	58	660	24	35.0	Sound o/p vs. mass flow/traverses.
	48	59	660	26.5	24.2	Sound o/p vs. mass flow/traverses.
	49	60	660	29	23.3	Sound o/p vs. mass flow/traverses.
	50	61	660	27.5		Anomaly/duct liner loose.
		62	660	27.5		Sound o/p vs. mass flow/traverses.
	51	63	660	25.8	33.3	Sound o/p vs. mass flow/traverses.
8/14/85	52	64	660	25.8	38.3	Baseline sound o/p run.
8/15/85	53	65	660	25.8	73.3	FRSI liner and internal baffles.
	54	66	660	25.8	73.3	FRSI liner.
	55	67	660	25.8	48.3	Internal baffles. Ref. vel. high.
		68	660	25.8		Internal baffles.
	56	69	660	25.8	40.0	Baseline sound o/p repeat.
	57	70	660	25.8	51.7	Open cell honeycomb side liner.
8/16/85	58	71	660	25.8		Flow deflector-downstream wall.
		72	660	25.8		Contamination screen traverse with deflec.
	59	73	660	25.8	43.3	Contamination screen traverse without deflec.

TABLE I.- Concluded

Date	Test Config. no.	Tape run no.	Duct velocity fps	Exit height in	Ref. velocity fps	Comments
8/21/85	60	74	660	25.8	41.7	Rubber streamers/8: 1.5 in. long.
	61	75	660	25.8	40.0	Rubber streamers/8: 1 in. long.
	62	76	660	25.8	45.0	Baseline sound o/p run.
		77	660	25.8		Anechoic treatment on room wall.
8/22/85	63	78	660	25.8	27.5	Two external B/L spoilers at 45°.
	64	79	660	25.8	24.2	Single castellated spoiler.
	65	80	660	23.4	30.0	Single castellated spoiler.
8/23/85	66	81	660	23.4	55.8	Anomalous run.
	67	82	660	25.8	52.5	Anomalous run.
8/26/85	68	83	660	25.8	6.7	Hardware cloth spoiler: 0.25".
	69	84	660	23.4	11.7	Hardware cloth spoiler: 0.25".
	70	85	660	21	18.3	Hardware cloth spoiler: 0.25".
	71	86	660	17.8	40.0	Hardware cloth spoiler: 0.25".
	72	87	660	21	43.3	Hardware cloth/fwd half opening.
	73	90	660	21	38.3	Hardware cloth/aft half opening.
	74	89	660	21	56.7	Hardware cloth/aft 4" opening.
	75	90	660	25.8		Rubber flap at opening/1.5" long.
	76	91	660	25.8	36.7	Rubber flap at opening/1.5" long.
	77	92	660	25.8	33.3	Rubber flap slit at center.
	78	93	660	25.8	11.7	External FRSI spoiler: 1" high.
	79	94	660	23.4	15.0	External FRSI spoiler: 1" high.
	80	95	660	19.2	38.3	External FRSI spoiler: 1" high.
	81	96	660	25.8		Flow traverse with 2" deflector.
	82	97	660	25.8		Flow traverse with 1" deflector.
	83	98	660	25.8	45.0	Sound directivity/baffle plate.
8/28/85	84	99	660	25.8	46.7	Baseline sound o/p run.
	85	100	660	25.8	43.3	FRSI streamers/2" long/0.32" thick.
	86	101	660	25.8	53.3	FRSI streamers/2" long/0.16" thick.
	87	102	660	25.8	53.3	FRSI streamers/2" long/0.32" thick.
	88	103	660	25.8	50.0	FRSI streamers/1.5" long/0.32" thick.
	89	104	660	28.5	33.3	FRSI streamers/1.5" long/0.32" thick.
	90	105	660	28.5	31.7	Baseline sound o/p run.

TABLE II.- VENT BOX MASS FLOW FOR DIFFERENT OPERATIONAL CONDITIONS

Tape run no.	Duct velocity, fps			Exit height, in	Duct pressures, psig			Mass flow, lb/s		
	Nom.	Max.	Avg.		Upstream <sup>a</sup>	Downstream <sup>a</sup>	Avg.	EMI	Screen	Total
7	200	212	190	11.5	0.058	0.193	0.126	0.808	2.415	3.223
8	200	218	189	13.1	.055	.088	.072	.459	1.813	2.272
9	200	212	188	15.0	.048	.050	.049	.201	1.002	1.203
11	350	386	349	15.5	.115	.058	.087	.164	1.485	1.649
13	350	386	346	13.9	.160	.300	.230	.566	2.785	3.351
16	350	385	348	13.1	.170	.318	.244	.696	3.176	3.872
19	350	383	346	15.0	.138	.173	.156	.275	2.035	2.310
22	500	550	538	16.2	.285	.215	.250	.236	2.213	2.449
24	500	556	524	16.9	.273	.075	.174	.303	1.689	1.992
26	500	561	529	18.0	.263	.148	.058	.357	1.615	1.972
28	500	560	526	20.0	.253	.315	.031	.330	.591	.921
30	500	552	524	15.0	.318	.515	.417	.319	2.694	3.013
32	500	552	520	13.3	.353	.698	.526	.700	3.581	4.281
72	660	(b)	(b)	25.8	.263	.658	.198	.321	.771	1.092
73	660	699	659	25.8	.273	.645	.186	.544	1.226	1.770
96	660	(b)	(b)	25.8	.395	.650	.128	.364	.609	.973
97	660	(b)	(b)	25.8	.388	.635	.124	.439	.757	1.196

<sup>a</sup>Upstream and downstream measurements are 5.75 inches forward and 4.37 inches aft of the vent opening, respectively.

<sup>b</sup>Duct cross-sectional mapping not done for this run.

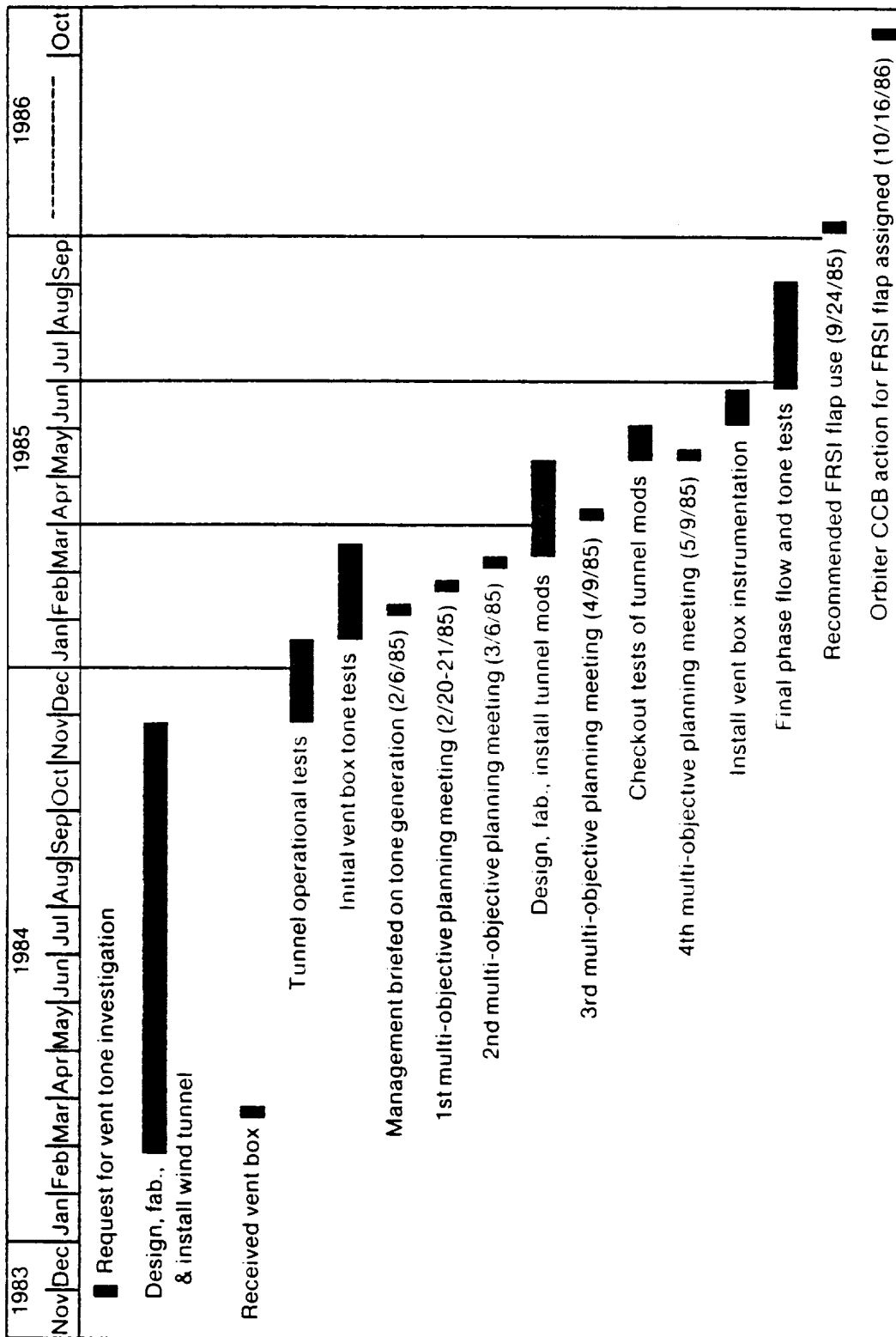


Figure 1.- Activity flow for payload bay atmospheric vent testing.

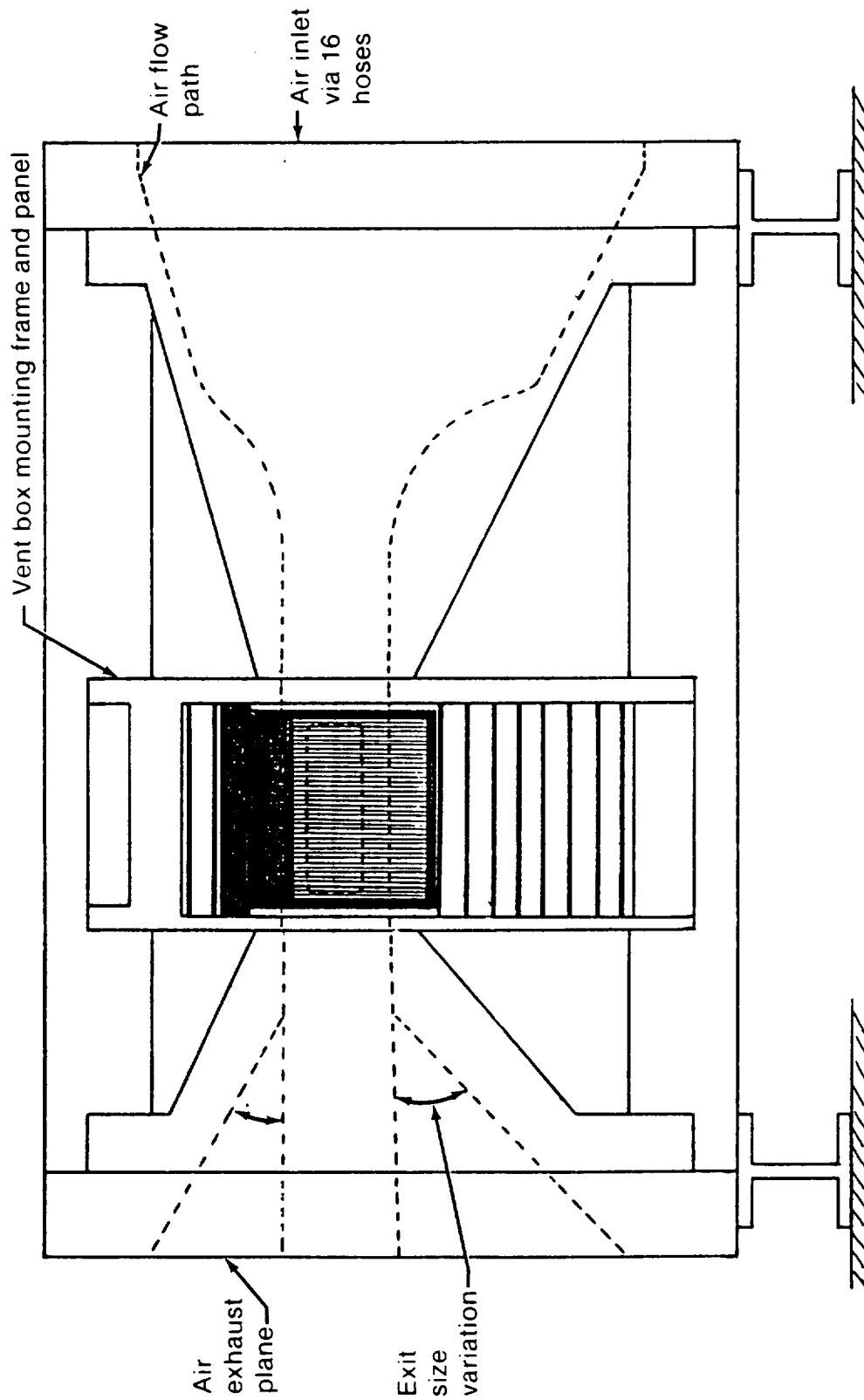


Figure 2.- Setup for Orbiter vent box wind tunnel tests.

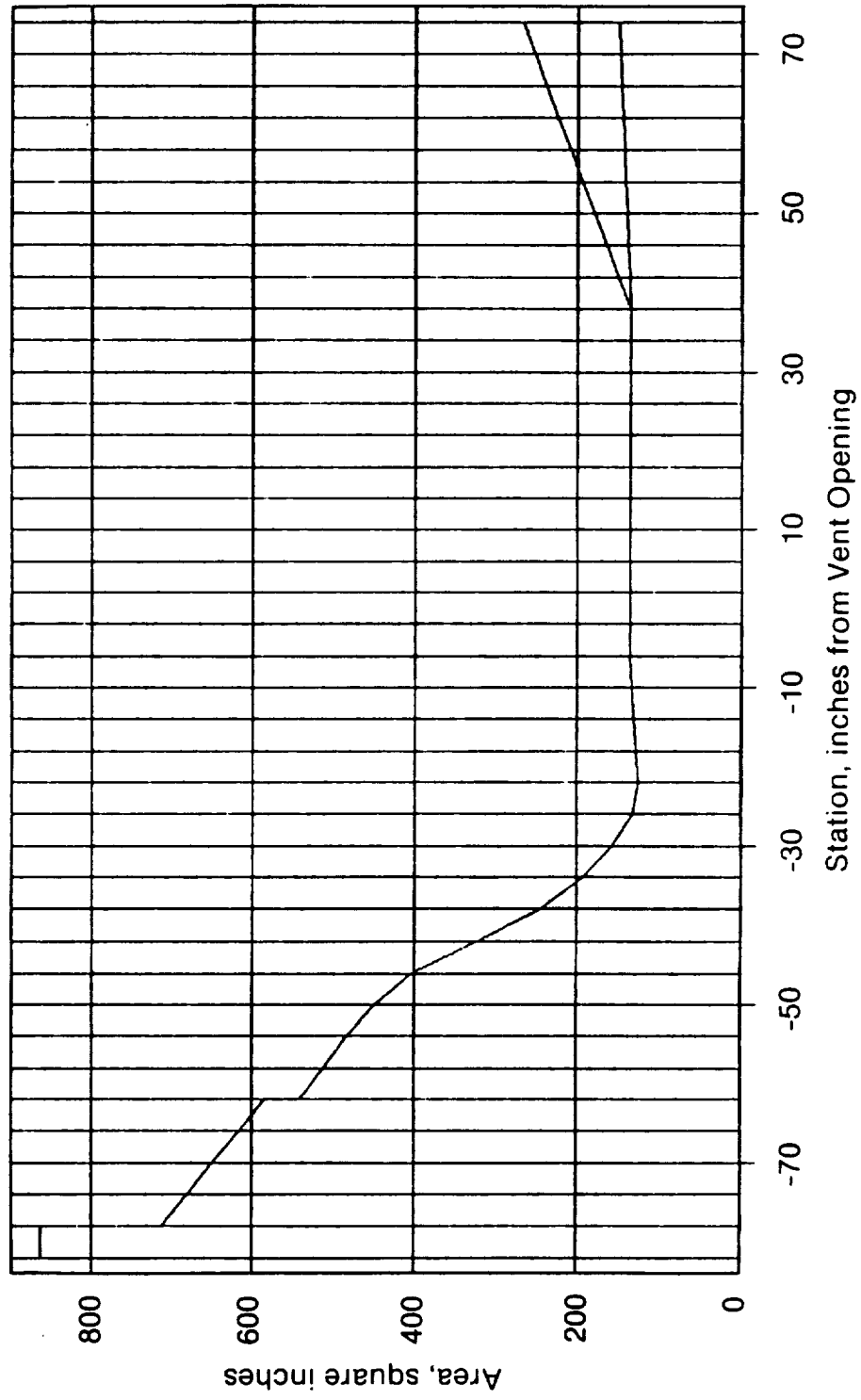


Figure 3.- Wind tunnel cross-sectional area versus axial station.



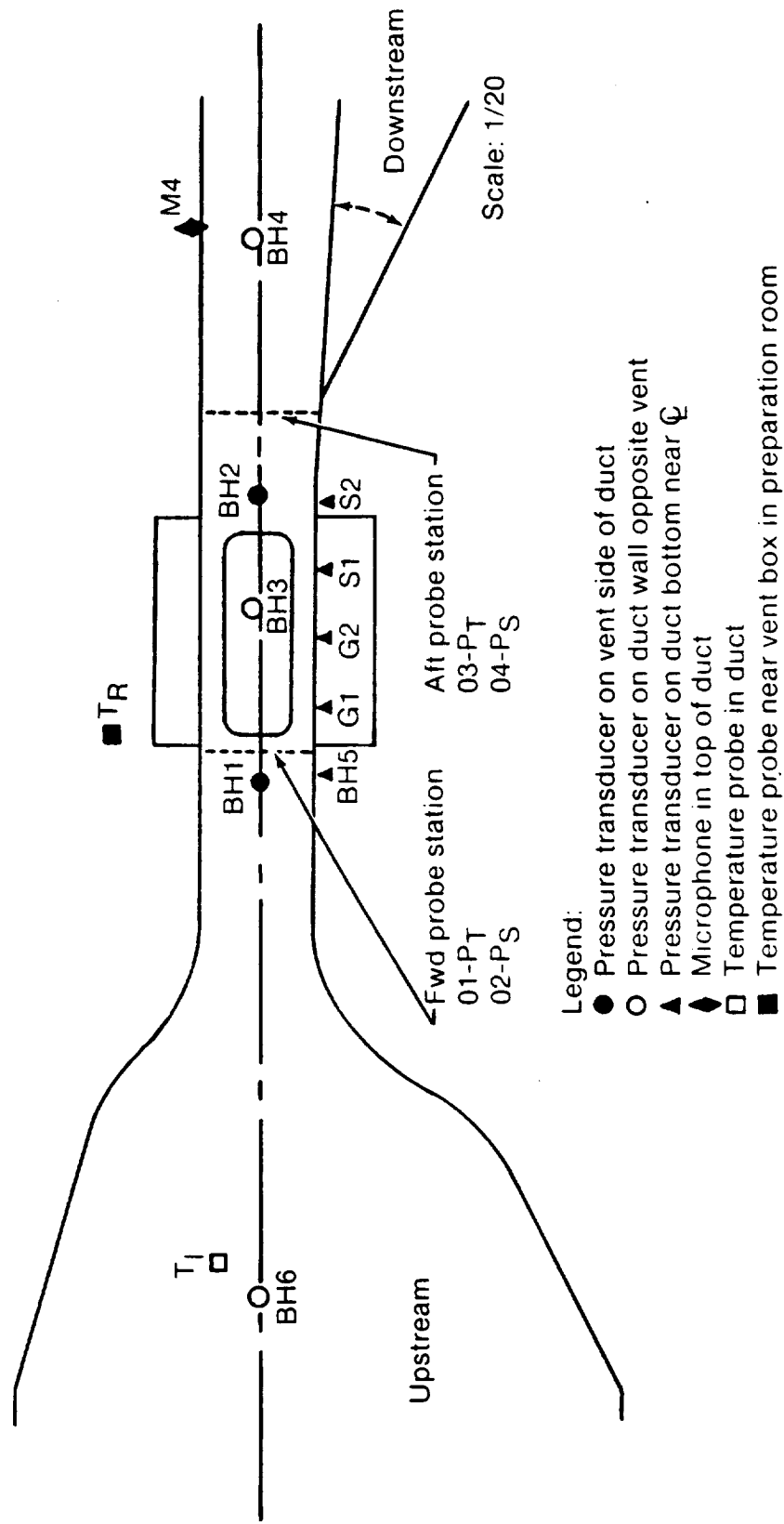
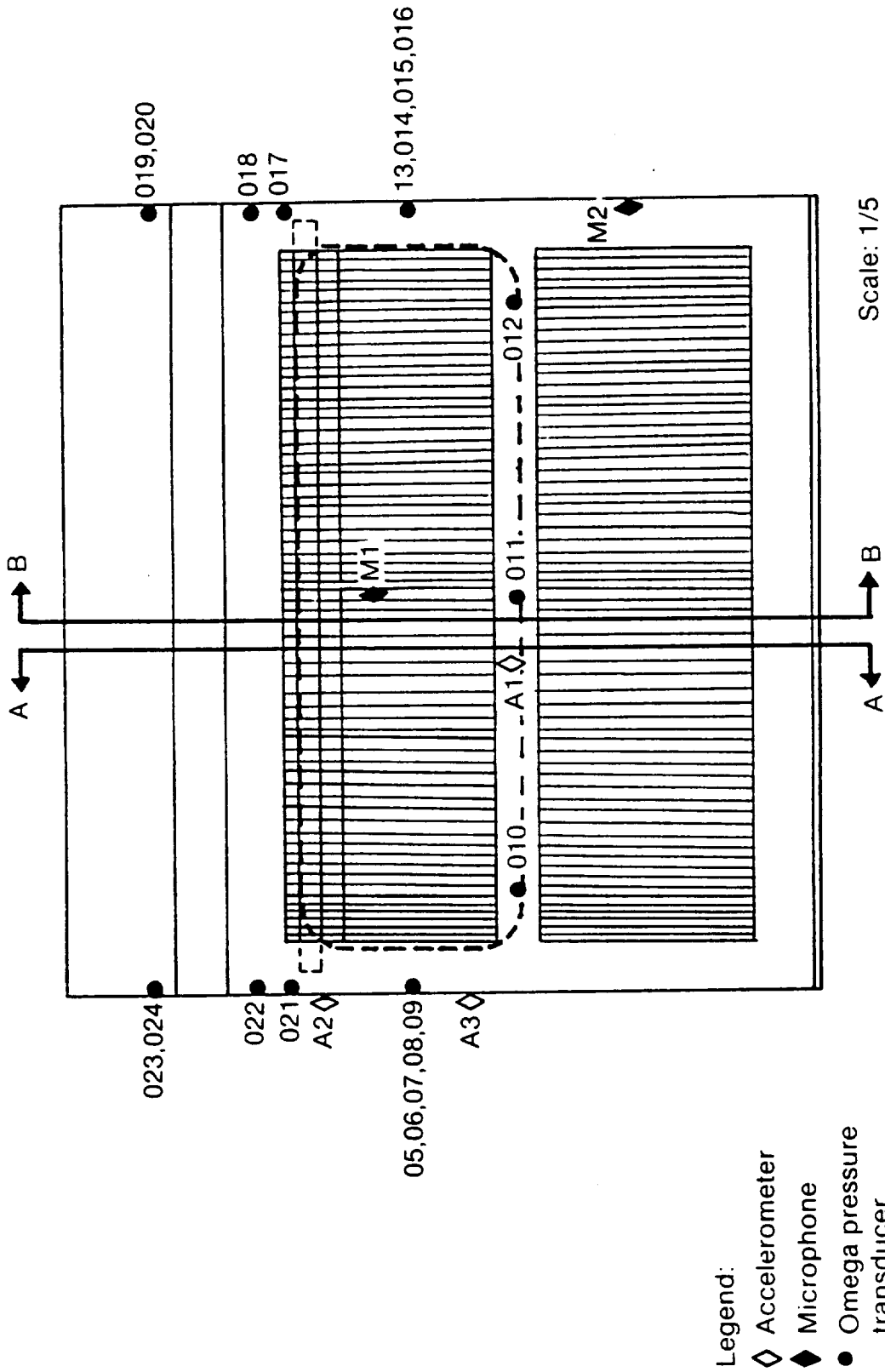
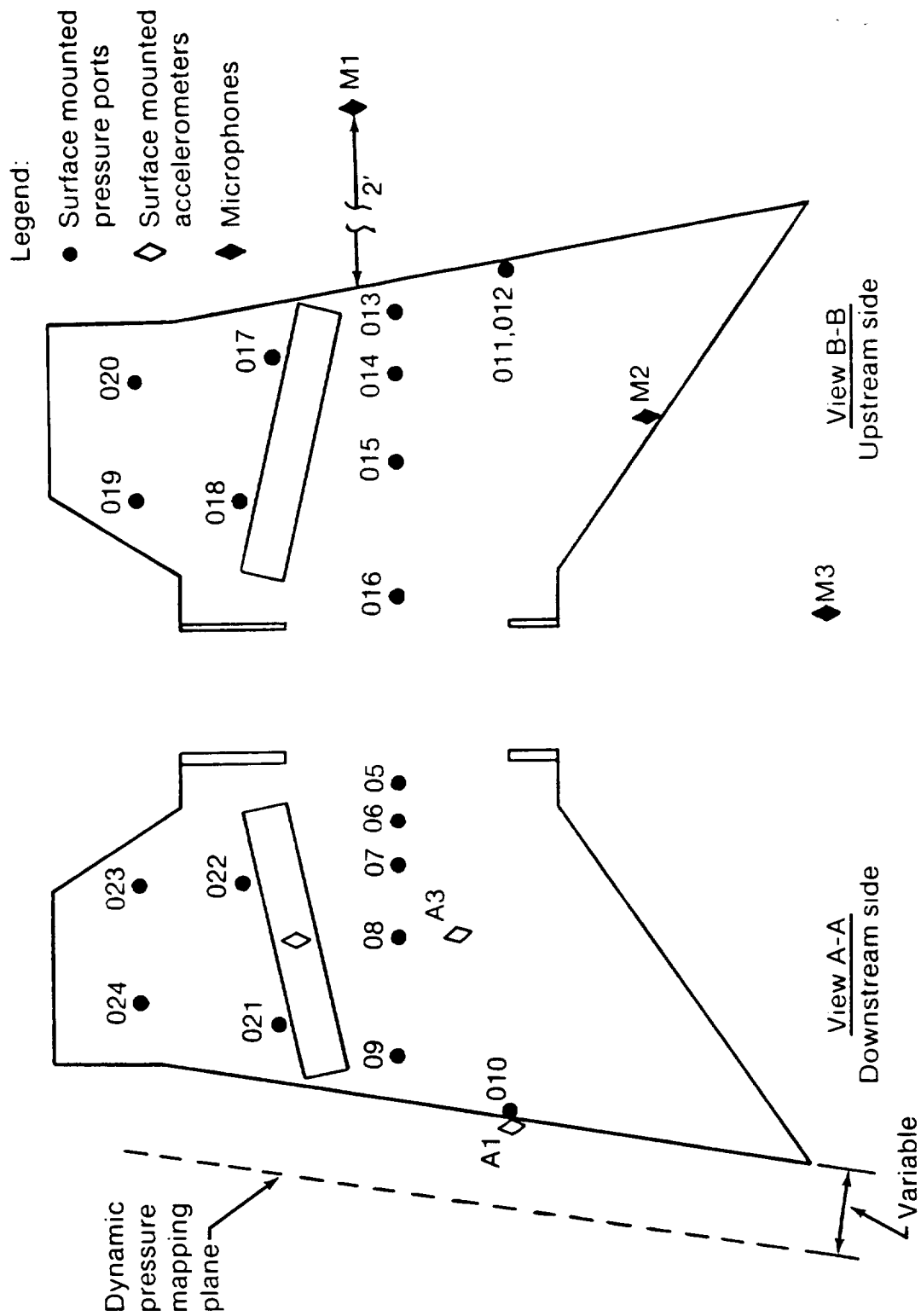


Figure 4.- Air path schematic for VATT wind tunnel showing fixed instrumentation locations.



(a) Front view.

Figure 5 - View of vent box showing instrumentation locations.



(b) Side views.

Figure 5. - Concluded.

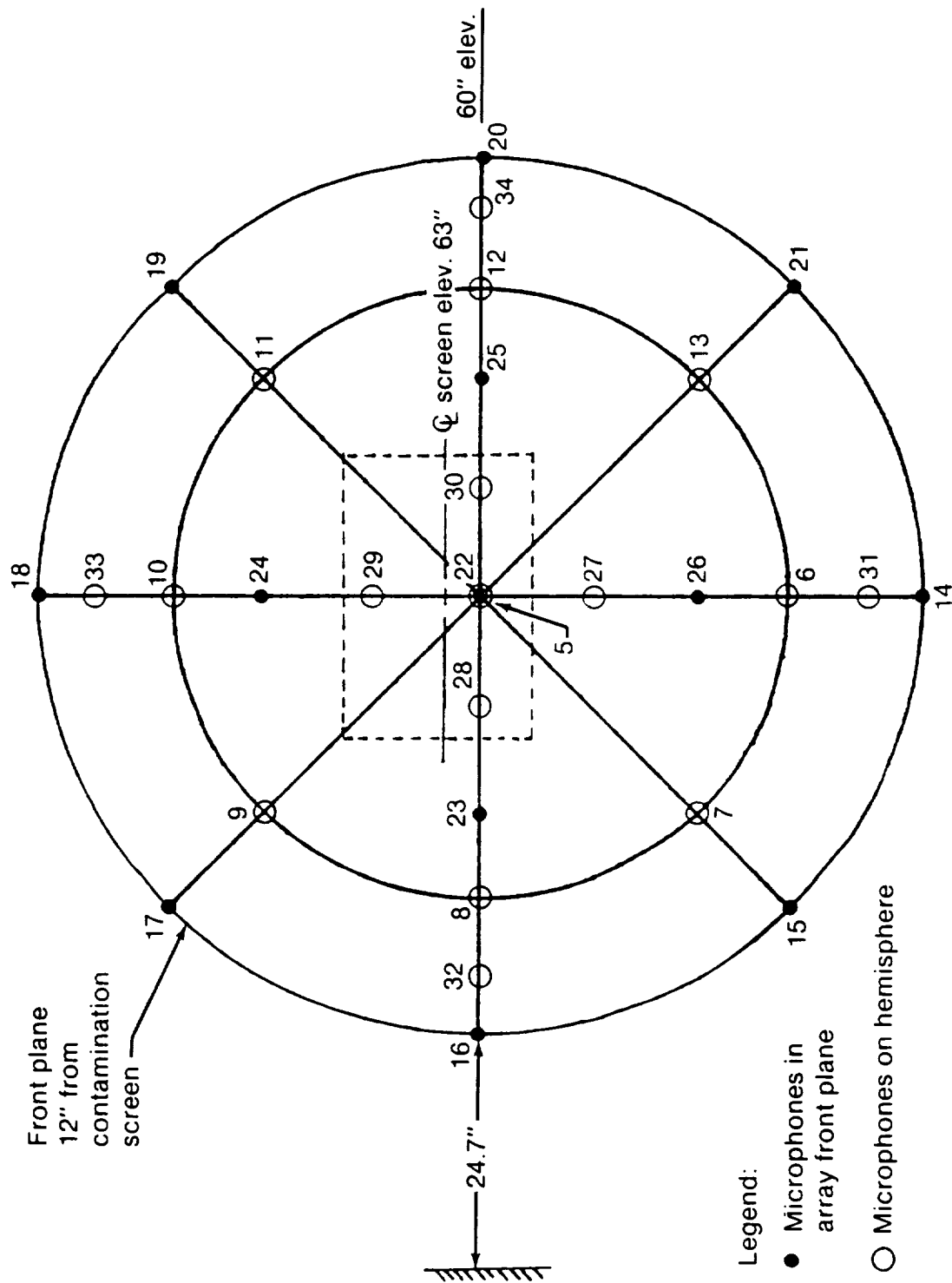


Figure 6.- Microphone array viewed from outside the hemisphere.

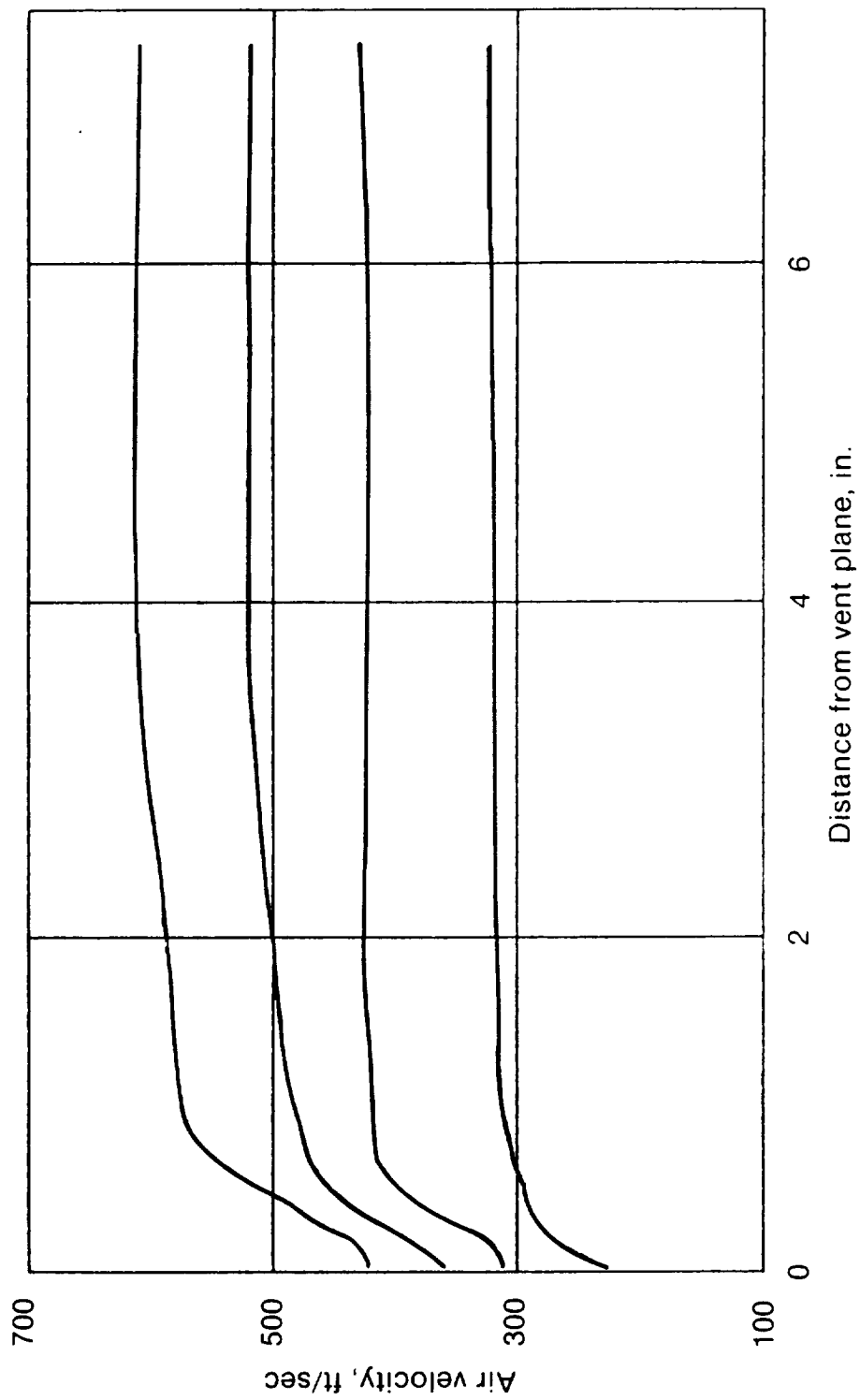
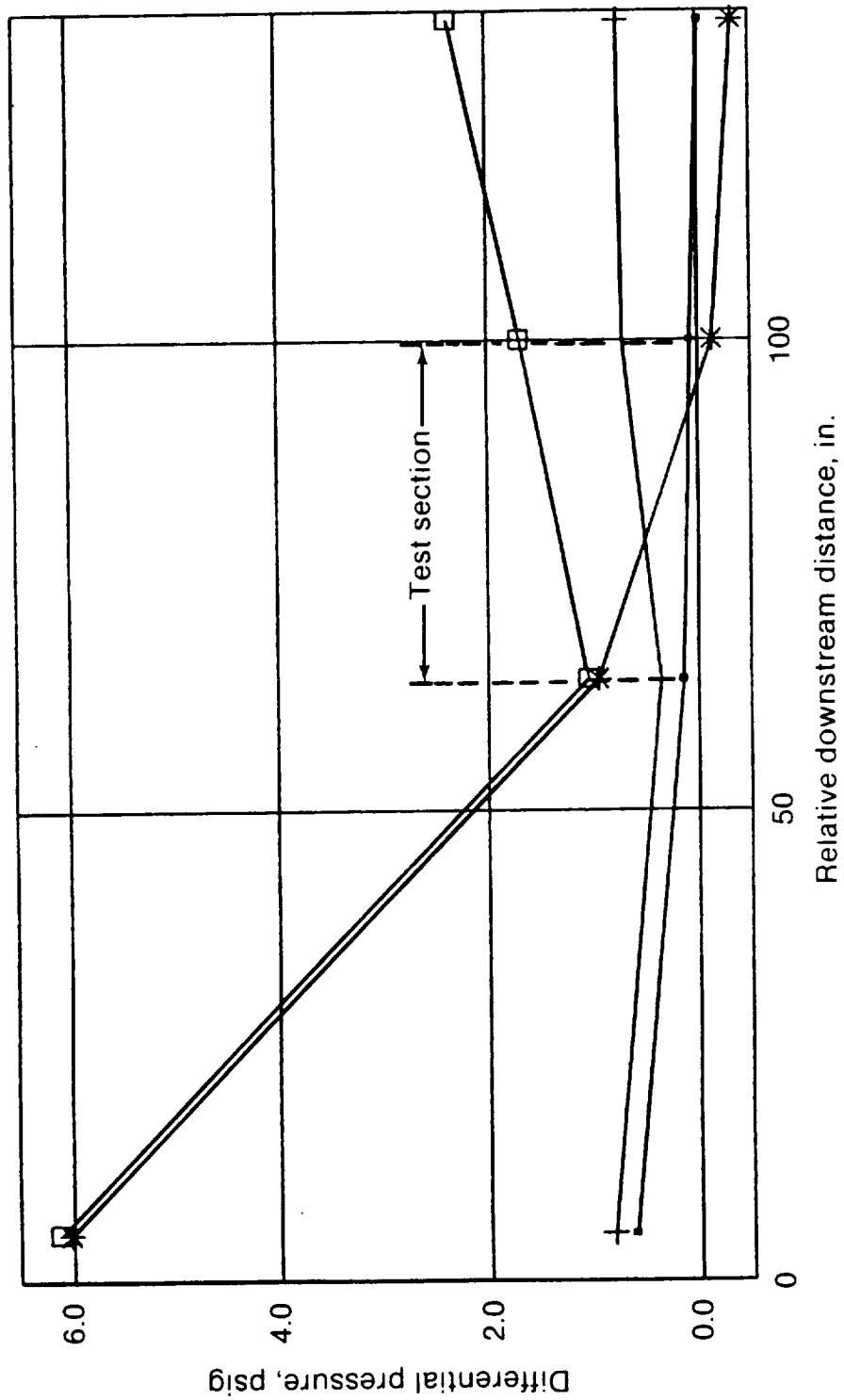


Figure 7. Velocity profiles across wind tunnel test section.



—●—  $V = 350, H = 16.2$  —+—  $V = 770, H = 16.2$  —\*—  $V = 350, H = 13.8$  —□—  $V = 770, H = 15.0$

Figure 8.- Control of static pressure by duct exhaust height variation.

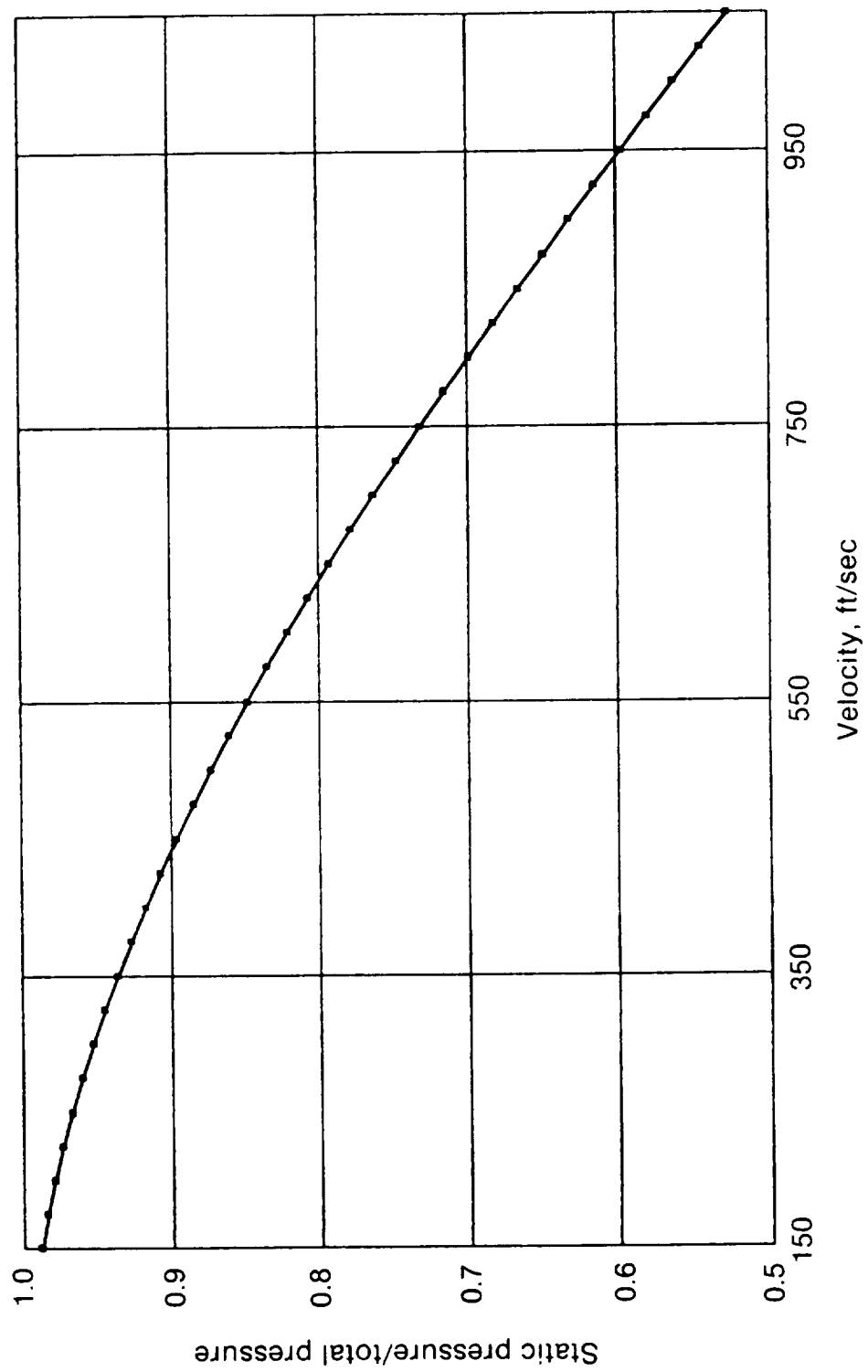


Figure 9 - Air velocity versus pressure ratio.

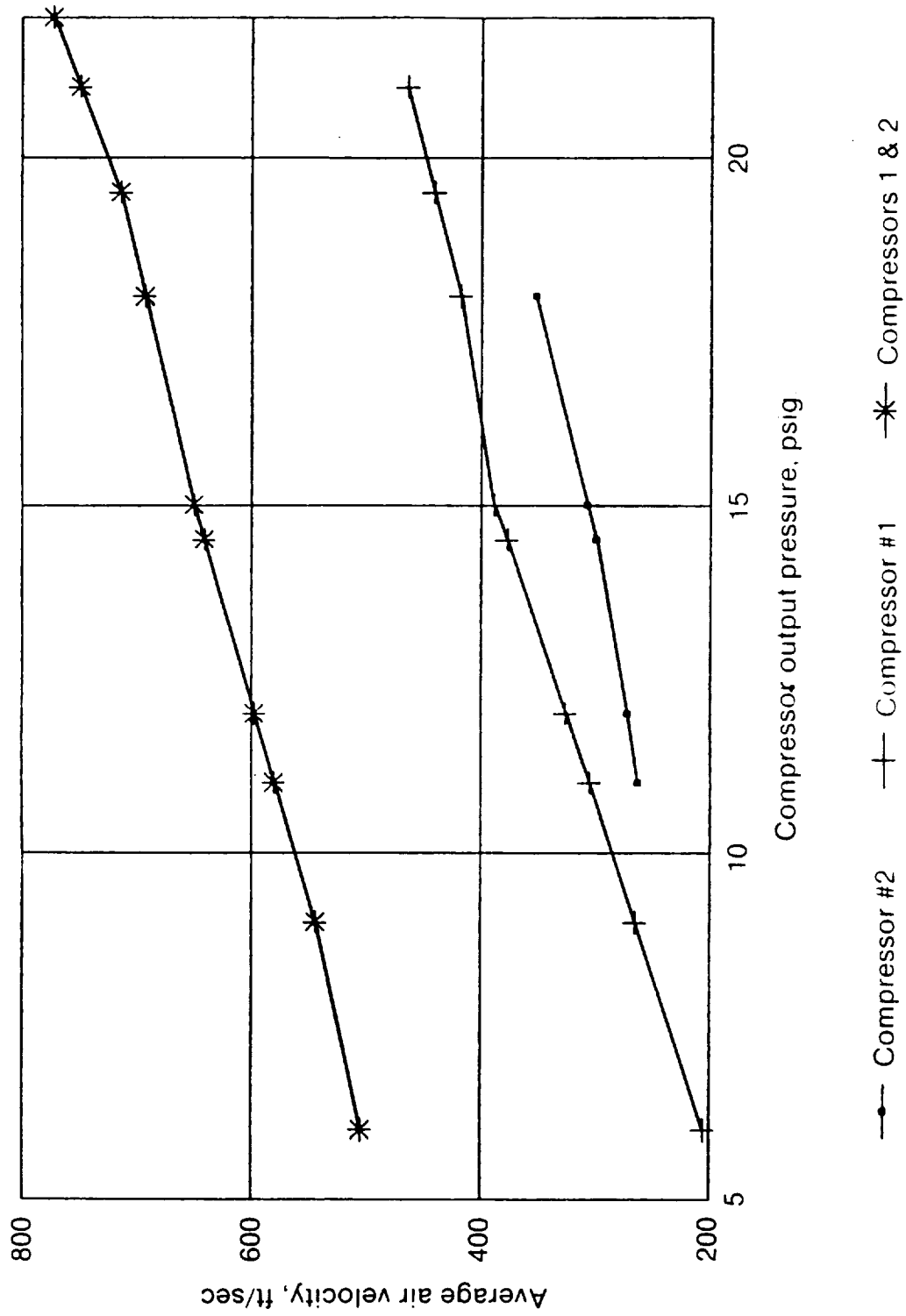


Figure 10. Average test section velocity versus compressor output pressure.



ORIGINAL PAGE IS  
OF POOR QUALITY

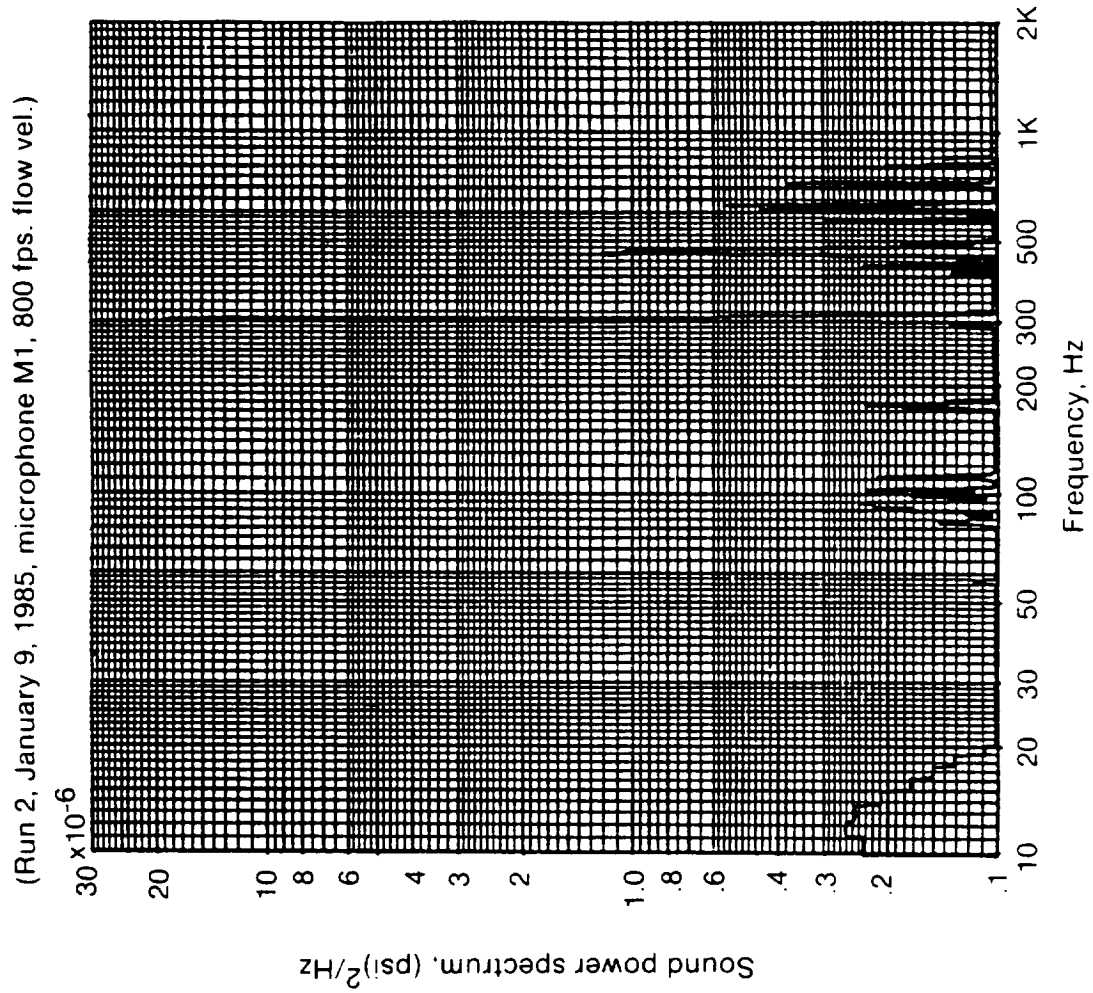
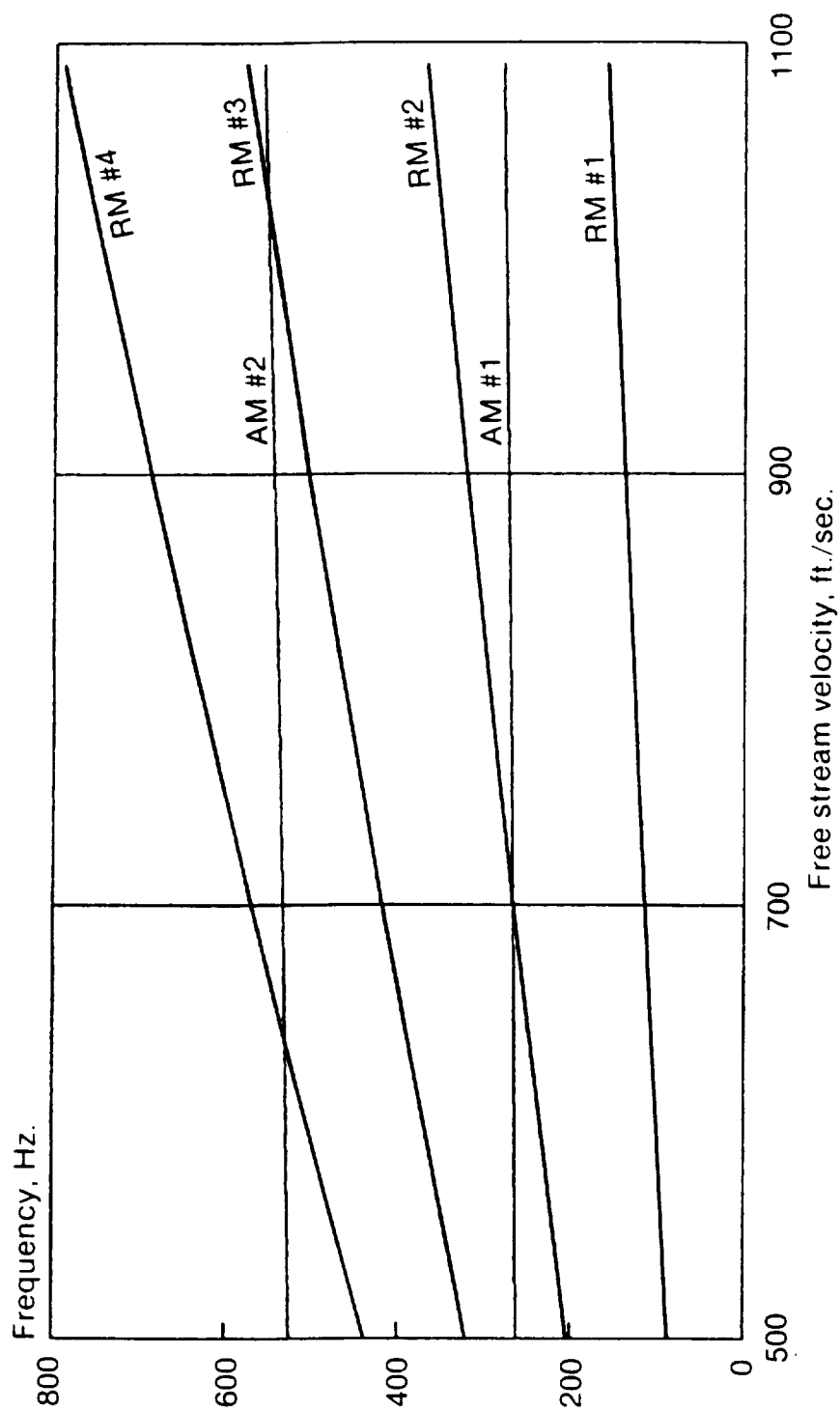


Figure 11.- Vent box tone generation in wind tunnel test at VATT.



Symbols:  
 RM# - rossiter mode number  
 AM# - acoustic mode number

Figure 12.- Overplot of Rossiter and acoustic modal frequencies versus velocity.

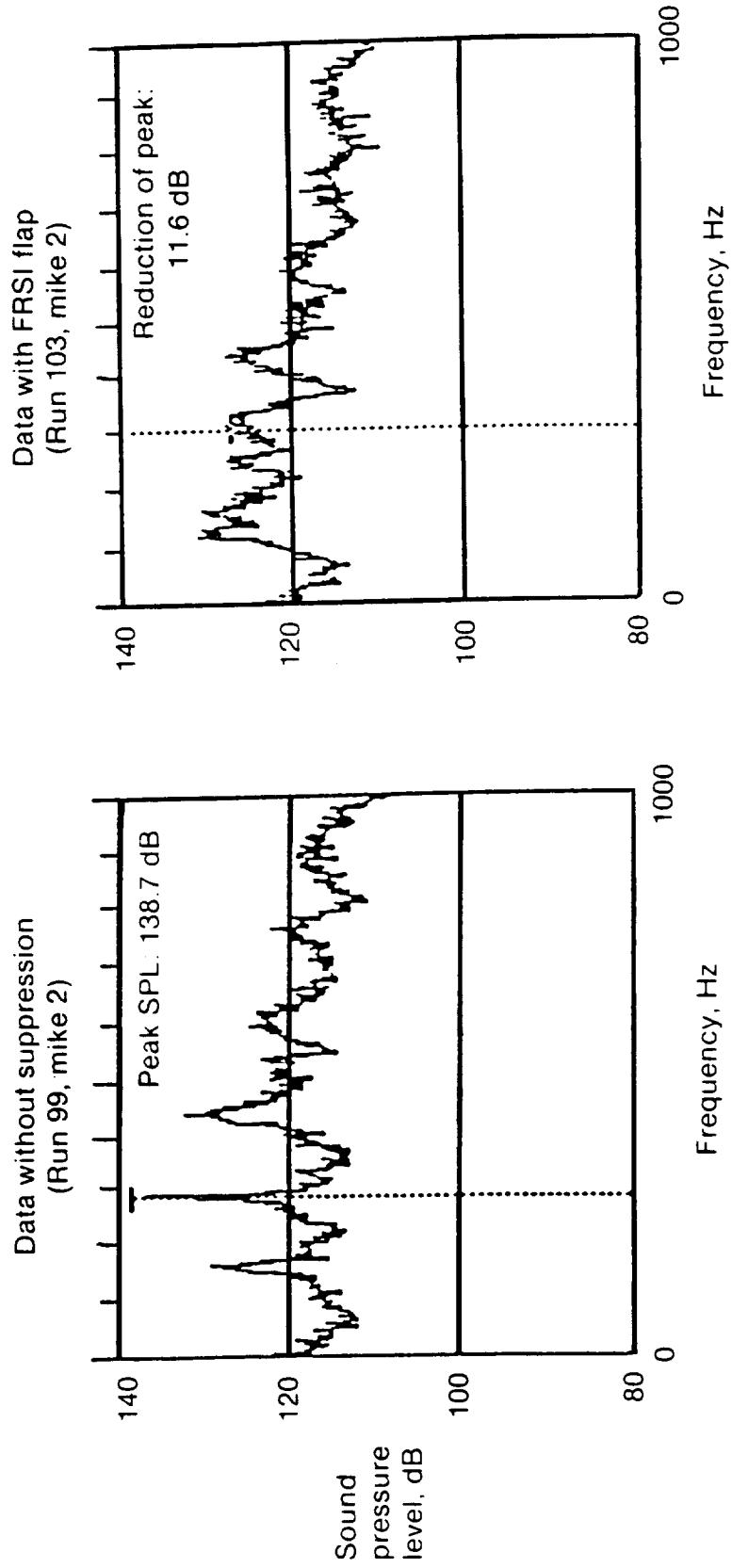


Figure 13. - Demonstration of dominant vent tone suppression by FRSI flap.

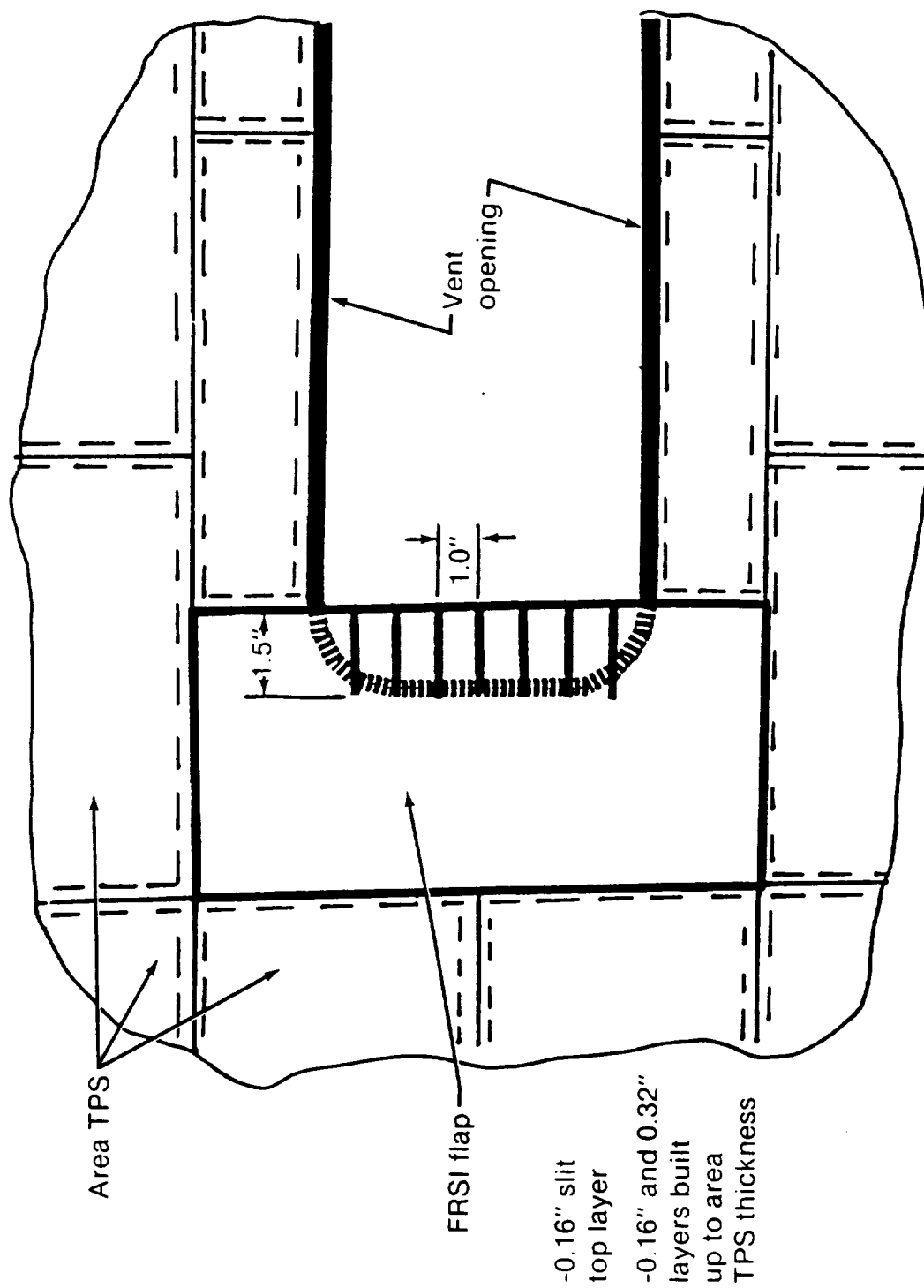


Figure 14.- Recommended FRSI flap configuration for payload bay vents 3, 4, and 5.

1. Report No. TM 100460		2. Government Accession No.		3. Recipient's Catalog No.	
4. Title and Subtitle Payload Bay Atmospheric Vent Airflow Testing at the Vibration and Acoustic Test Facility				5. Report Date February 1988	
				6. Performing Organization Code	
7. Author(s) James D. Johnston, Jr.				8. Performing Organization Report No. S-572	
				10. Work Unit No. 992-15-00-00-72	
9. Performing Organization Name and Address Lyndon B. Johnson Space Center Houston, Texas 77058				11. Contract or Grant No.	
				13. Type of Report and Period Covered Technical Memorandum	
12. Sponsoring Agency Name and Address National Aeronautics and Space Administration Washington, D.C. 20546				14. Sponsoring Agency Code	
15. Supplementary Notes					
16. Abstract  Several concerns related to venting the Space Shuttle Orbiter payload bay during launch led to laboratory experiments with a flight-type vent box installed in the wall of a subsonic wind tunnel. This report describes the test setups and procedures used to acquire data for characterization of airflow through the vent box and acoustic tones radiated from the vent-box cavity. A flexible boundary-layer spoiler which reduced the vent-tone amplitude is described.					
17. Key Words (Suggested by Author(s))  boundary layer spoiler airflow over cavities cavity tones payload bay vents			18. Distribution Statement  Unclassified - Unlimited   Subject Category: 02		
19. Security Classif. (of this report) Unclassified	20. Security Classif. (of this page) Unclassified	21. No. of pages 29	22. Price*		

